Repulsive Wall Effects Leading to Graduated Core-Shell Supramolecular Structure in Polystyrene Latexes

Se-In Yang,[†,‡,§] A. Klein,[†,‡] and L. H. Sperling*[,†,‡,§,∥]

Center for Polymer Science and Engineering, Department of Chemical Engineering, Materials Research Center, and Department of Materials Science and Engineering, Whitaker Laboratory No. 5, Lehigh University, Bethlehem, Pennsylvania 18015

E. F. Casassa

Department of Chemistry, Carnegie Mellon University, 4400 Fifth Avenue, Pittsburgh, Pennsylvania 15213

Received February 3, 1989; Revised Manuscript Received April 2, 1990

ABSTRACT: The factors controlling the core-shell supramolecular structure inside latex particles were investigated in a seeded styrene emulsion polymerization by small-angle neutron scattering (SANS). Seed latexes of deuterated polystyrene (polymer I) were swollen with an equal weight of protonated styrene monomer (monomer II) and equilibrated. Latex particles of about 700-800 Å in diameter contained polymers with weight-average molecular weights ranging from 2×10^4 to 8×10^5 g/mol. SANS measurements were done on the latex dispersions in the swollen state, at intermediate conversion, and after the complete conversion of the second-stage polymerization. The existence of segregation was identified as highest in the swollen state and decreasing somewhat as polymerization proceeds. The particle-water interface can be described as a repulsive wall in the de Gennes and Cassasa sense, leading to a concentration gradient of polymer I. This produces a polymer-rich core surrounded by monomer-rich shell. Both SANS results and the theoretical segment density profile indicate that the extent of segregation depends on the relative ratio of the chain radius of gyration to the particle radius, going through a maximum when this ratio becomes about 0.2. The kinetics of emulsion polymerization should be modified to allow for the repulsive wall effect and concomitant segregation.

Introduction

Earlier theoretical treatments of emulsion polymerization have generally assumed that partly polymerized particles were swollen uniformly with monomer, monomer and polymer being fully miscible in all proportions and homogeneous. However, the field has also been controversial. Williams and co-workers[1-4] postulated a core-shell model in which a monomer-rich shell surrounds a polymer-rich core under equilibrated swelling conditions, the outer shell serving as the major locus of polymerization. On the contrary, Gardon and others presented kinetic evidence for uniformly swollen latex particles.[5-7]

For polymer solutions Casassa and Tagami,[8,9] de Gennes,[10-12] and Richmond and Lal[13] estimated the reduction in entropy of chain arrangements inside a confined geometry, describing the interface as a repulsive wall. This results in a depleted polymer layer near the wall. They found that the reduction in entropy depends on the chain dimensions and the confining geometry. Allain et al.[14] demonstrated the existence of a depletion layer near the repulsive wall by optical observation.

Small-angle neutron scattering (SANS) can be applied to latex systems to examine chain conformation, the extent of molecular segregation, and other morphological features inside the particle, as in the case of bulk systems.[15-17] The necessary contrast for SANS is provided by substituting deuterium for hydrogen in probe polymer chains without significantly altering the chemistry of the system under investigation.

Linne et al.[18,19] first showed the existence of molecular segregation in polystyrene latexes via SANS, important variables being the molecular weight of the polymer and the particle size. Linne et al.[18,19] also found that polymer chains having high molecular weight are constrained inside a relatively small-sized particle, because the relaxed chain dimensions are much larger than the particle size. Under these conditions, uniform molecular mixing was thought as forced mixing due to the reduced entropy. In the previous paper in this series,[20] molecular segregation was investigated by SANS. The final morphology of the polystyrene latex varied from uniform molecular mixing to that of considerable supramolecular structure, depending on the relative ratio of chain dimensions to the particle diameters.

However, the formation mechanism of supramolecular structures such as possible core-shell morphologies is not yet clear on a quantitative basis. There are two possibilities of core-shell morphologies in the final latex particles. One is a diffusion-controlled kinetic mechanism. The newly formed polymer molecules are likely to be close to the particle surface even though the monomer is distributed uniformly throughout the particle, because the monomer diffuses to the site of polymerization and the polymer moves only by addition of monomer molecule.[21] The other model involves a polymer-rich core and a monomer-rich shell in the swollen state, with the concentration gradient remaining during the polymerization of the added monomer. This segregation was ascribed to the very bad mixing thermodynamics of having chain loops and ends protrude into an aqueous phase.[18-20]

In this paper, the formation process of supramolecular structures is considered. The seed particles are composed of deuterated polystyrene (polymer I). A series of seeded styrene emulsion polymerizations was prepared by varying the molecular weight of the polymer I and the amount of styrene (monomer II). SANS measurements were done in the equilibrium swollen state, at intermediate conversion, and after the complete conversion of the added protonated styrene. The segregation process is thought

[†] Center for Polymer Science and Engineering.
[‡] Department of Chemical Engineering.
[§] Materials Research Center.
[∥] Department of Materials Science and Engineering.

0024-9297/90/2223-4582$02.50/0

to arise from the "repulsive wall" effect of Casassa[8,9] and de Gennes.[10-12] This strengthens the thermodynamic mixing approach and provides ready-made analytical methods to quantitatively describe the depleted layer.

Theory for SANS

The SANS technique can be used to measure both domain sizes and individual chain dimensions with such domains in multiphase systems. The general equation for the coherent scattering cross section in an incompressible blend of two-phase systems can be described as the simple addition of the domain scattering and the molecular scattering, which is given by the cross section $d\Sigma/d\Omega$,[17] which is the probability that a neutron will be scattered in a solid angle, Ω, per unit volume of the sample. Thus

$$\frac{d\Sigma}{d\Omega}(\mathbf{K}) = X(1-X)(a_H - a_D)^2 N_p P_1(\mathbf{K}) + \left[a_H(1-X) + a_D X - a_s\frac{V_p}{V_s}\right]^2 \frac{P_T(\mathbf{K})}{V} \quad (1)$$

where subscripts p and s represent the p species and the s species, respectively, $\mathbf{K}$ represents the momentum transfer vector ($\mathbf{K} = (4\pi/\lambda)\sin(\theta/2)$) where λ is the neutron wavelength and θ is the scattering angle, X is the deuterated mole fraction of the p species, a_H and a_D are the respective scattering lengths of protonated and deuterated structural unit, $N_p = (\rho N_A M_w \phi/m_D^2)$, ρ and M_w are the density and the weight-average molecular weight of the p species, N_A is Avogadro's number, ϕ is the volume fraction of the p species in the sample, m_D is the molecular weight of the deuterated monomer, a_s is the scattering length of a structural unit of the s species, V_p and V_s are the monomer molar volumes of the p and s species, and V is the total sample volume. The quantity $P_T(\mathbf{K})$ is proportional to the total scattering from a blend where the p species is fully deuterated ($X = 1$) and can be analyzed to give the dimensions of the individual phase structure. The quantity $P_1(\mathbf{K})$ is the Debye single-chain form factor given by

$$P_1(\mathbf{K}) = \frac{2}{(\mathbf{K}R_g)^4}[(\mathbf{K}R_g)^2 - 1 + \exp(-\mathbf{K}^2R_g^2)] \quad (2)$$

where R_g is the radius of gyration for a single chain.

Bates et al.[22-25] studied single-chain scattering in a polystyrene-*block*-polybutadiene diblock copolymer system by selecting a suitable value of X for the p species so that the quantity in the square brackets of the second term of eq 1 is zero. This condition is known as the phase-contrast matching condition. They found a higher level of scattering than predicted for uniform molecular mixing inside the phase domains, especially in the lower angular range of the SANS data, and concluded that the deuterated polybutadiene chain portions undergo clustering in the spherical domains.

Latex systems display a distinct similarity in scattering behavior to block copolymers; i.e., they constitute multiphase systems due to the existence of the aqueous phase and the soap surrounding the latex particles. The soap effect, other extraneous interfacial effects, incoherent scattering, etc., can be corrected by appropriate blank subtraction.[26,27] After blank correction, the second term of eq 1 can be replaced by the spherical scattering of latex systems. Thus, the total scattering cross section can be given by[20]

$$\frac{d\Sigma}{d\Omega}(\mathbf{K}) = X(1-X)(a_H - a_D)^2 N_p P_1(\mathbf{K}) + A[\rho_{mH}(1-Y) + \rho_{mD}Y - \{\rho_D X + \rho_H(1-X)\}]^2 \phi_R V_R P_2(\mathbf{K}) \quad (3)$$

where A is a SANS calibration constant, Y is the mole fraction of D_2O in the aqueous phase, ρ_{mH} and ρ_{mD} are the scattering length densities of H_2O and deuterium oxide, ρ_H and ρ_D are the scattering length densities of protonated and deuterated polymer, respectively, ϕ_R is the volume fraction of the latex particles having radius R, and V_R is the volume of the particle ($V_R = (4/3)\pi R^3$). In some of the present systems, the monomer, styrene, is present in various amounts. The extension of eq 3 to the case where monomer (or solvent) is present[27b] is discussed in Appendix I.

The quantity $P_2(\mathbf{K})$ is the spherical-scattering form factor given by

$$P_2(\mathbf{K}) = \left[\frac{3(\sin(\mathbf{K}R) - \mathbf{K}R\cos\mathbf{K}R)}{(\mathbf{K}R)^3}\right]^2 \quad (4)$$

When the quantity X in eq 3 equals zero or unity, eq 3 represents only spherical scattering. Several studies characterized the core–shell structure in latex particles of immiscible systems by contrast matching of the core or the shell with the aqueous medium.[28-30]

Like the block copolymer systems studied by Cohen and co-workers,[22-25] the single-chain dimensions inside latex particles can be determined on the basis of contrast matching between the aqueous medium and the particles by using the appropriate mixture of D_2O and H_2O. When the average contrast factor of the aqueous medium is matched to that of the particle in which deuterated and protonated chains are uniformly mixed, the second term of eq 3 will cancel out, leaving only the single-chain scattering.

However, when there is a concentration gradient of deuterated and protonated chains or molecular segregation exists inside the particle, the second term of eq 3 will not vanish completely, because the contrast between the aqueous medium and the particle cannot be truly matched. Neither of the terms in eq 3 exactly represents the scattering from the supramolecular structure. In this case, the zero-angle scattering intensity, $[d\Sigma/d\Omega](0)$, reflecting molecular segregation, will be much higher than expected on the basis of uniform molecular mixing inside the particle. Hasegawa et al.[31] and Matsushita et al.[32] studied the contrast mismatching caused by concentration fluctuations in a mixture of protonated and deuterated polystyrene inside the lamellar structure, but the exact equations that account for the concentration gradient quantitatively have not been derived.

The present paper studies the molecular segregation inside latex particles under different contrast matching conditions between the aqueous medium and the particle. The most important quantity is the zero-angle scattering intensity, $[d\Sigma/d\Omega](0)$, which is proportional to the number of segregated chains per particle.

Guinier has shown that the scattering from any isotropic substance, including spherical scattering, can be approximated in the low-angle region by an exponential function. According to Guinier approximation, eq 3 in the low-angle region ($\mathbf{K}R_g \ll 1$) can be expressed by[33]

$$\frac{d\Sigma}{d\Omega}(\mathbf{K}) = \frac{d\Sigma}{d\Omega}(0)\exp(-\mathbf{K}^2R_g^2/3) \quad (5)$$

For a sphere, radius a is related to the radius of gyration,

R_g:

$$a^2 = (5/3)R_g^2 \tag{6}$$

The quantity, $[d\Sigma/d\Omega](0)$, is determined at zero angle by plotting ln $[[d\Sigma/d\Omega](\mathbf{K})]$ vs $\mathbf{K}^2$, a linear relation being expected.

The quantity N_s is defined as the extent of segregation

$$N_s = \frac{\left[\frac{d\Sigma}{d\Omega}(0)\right]_{SANS}(\text{exptl})}{\left[\frac{d\Sigma}{d\Omega}(0)\right]_{GPC}(\text{calcd from GPC})} \tag{7}$$

where $[[d\Sigma/d\Omega](0)]_{GPC}$ is calculated from the GPC experimental molecular weight. It represents the theoretical value that would be obtained when there is uniform molecular mixing inside the particle. It is calculated by using the first term of eq 3, substituting the known molecular weight determined by GPC.

For bulk polystyrene, the radius of gyration for single chains depends on the molecular weight by[34,35]

$$R_g = 0.275M_w^{1/2} \tag{8}$$

and the chain end-to-end distance by

$$\bar{r} = \sqrt{6}R_g = (0.674)M_w^{1/2} \tag{9}$$

For large chains in small latex particles, some of the examples treated below, R_g and $\bar{r}$ are reduced or constrained by the actual size of the latex particle.

Experimental Section

All latex particles were prepared by a seeded emulsion polymerization by using a bottle polymerization technique. The protonated and deuterated styrene monomers (Aldrich Co. and Cambridge Isotope) were purified by removing the inhibitors on neutral alumina and stored at 4 °C until used. The water (H_2O) was doubly distilled, and the deuterium oxide (D_2O, 99%) was used as received (Chemical Dynamics Co.). A seed latex composed of deuterated polystyrene was synthesized in the first step at 60 °C. The formulations were based on a 36-g mixture of the D_2O and H_2O for the aqueous phase, the composition of the deuterium oxide being variable in each series of experiments as explained below; 2 g of deuterated styrene monomer, 0.06 g of sodium lauryl sulfate (anionic surfactant), 0.6 g of Triton X-100 (nonionic octylphenoxyethyl surfactant; Rohm and Haas Co.), 0.1 g of potassium persulfate (initiator), and 0.015 g of potassium hydroxide (pH regulator). The molecular weight of the seed latex within each series was varied by adding carbon tetrachloride as a chain-transfer agent.

After the seed latex of deuterated polystyrene was synthesized, protonated styrene monomer was added and 48 h was allowed to swell the latex particles to equilibrium. No additional polymerization occurred during this time.

The molecular weights of the seed particles were analyzed by gel permeation chromatography (Waters), being taken by the average of three measurements. The swollen particle sizes were analyzed by a photon correlation spectrophotometer (Coulter N_4), and transmission electron microscopy, TEM (Philips 300), was used to characterize the particle size and its distribution on the seed and after completion of the polymerization of the added monomer. The Coulter N_4 values averaged slightly larger than the TEM values, by approximately the difference in density between the partially and fully polymerized latexes.

The SANS experiments were performed on the SANS facility at the National Bureau of Standards. A neutron wavelength of 8.0 Å and a sample-to-detector distance of 3.6 m were used. A multibeam-converging collimation system was used to increase the neutron intensity on the sample. All latex samples, including the blanks, were diluted to 5% solid content and placed in liquid spectroscopy quartz cells having 0.2-cm pathways. Calibration of the SANS instrument was done by silica gel absolute intensity standard. In all cases, the recorded intensities for the samples and the blanks were radially averaged and converted to absolute values through a calibration constant. The coherent intensities of the samples were obtained by subtracting the intensities of the corresponding blanks.

Table I
Sample Characterization

sample ID	mol wt of seed latex polym M_n(GPC) $\times 10^{-3}$	mol wt of seed latex polym M_w(GPC) $\times 10^{-3}$	seed radius (a_w), Å	particle radius (a_w, Å) molar swelling ratio 1.0[a]	2.0	3.0
S-1	250	800	295	365		
S-2	130	404	295	365	425	480
S-3	110	320	295	365		
S-4	62	200	305	380		
S-5	28	100	305	380		
S-6	16	58	305	390	440	495
S-7	12	40	330	410		
S-8	6	20	410	505		

[a] 100% swelling by new monomer.

Table II
SANS Studies on Swollen Latex Particles before Polymerization

sample ID	latex scaling ratio (R_g/a_w)	extent of segregation (N_s)
S-1	0.68	21
S-2	0.48	43
S-3	0.42	43
S-4	0.32	61
S-5	0.23	89
S-6	0.17	100
S-7	0.14	83
S-8	0.08	31

Table III
SANS Studies on the Latex Particle during and after the Polymerization

sample ID	latex scaling ratio (R_g/a_w)	conversn, %	extent of segregation (N_s)
S-2	0.48	0	43
I-2	0.48	42	12
C-2	0.48	>98	10
S-4	0.32	0	61
I-4	0.32	42	30
C-4	0.32	>98	23
S-6	0.17	0	100
I-6	0.17	42	35
C-6	0.17	>98	20

Final latex samples for SANS analysis were prepared as follows.

Contrast Matching to the Whole Swollen Polymer Particle. Series S Samples. The composition of the swollen latex particles was 50/50 mol % of deuterated polystyrene and protonated styrene monomer (1:1 molar swelling ratio). With the mixture of D_2O/H_2O (64/36 mol %), the average contrast factor of the aqueous medium was matched to that of the swollen latex particle. A master batch of D_2O/H_2O was used for all samples and blanks to reduce minor errors from experimental composition changes. After equilibration, the series S samples were prepared in the swollen state without further polymerization; see Tables I and II.

Series I Samples. In the series I samples, the swollen latex particles were allowed to react partially by stopping the polymerization in the intermediate stage by quenching the temperature, the unreacted monomer being left inside the latex particles; see Table III.

Series C Samples. In the series C samples, the polymerization of the swollen latex particles was continued to complete conversion; see Table III. The conversion was determined by gravimetric analysis. Molecular weights were determined via GPC on the seed latexes and after final conversion. The results are shown in Table IV. As in the previous paper,[20] the final molecular weights are close to the seed molecular weights.

Table IV
Molecular Weights of Polymers in Seed and Final Latex Particle

	seed latex		final latex	
sample ID	M_w(GPC) × 10^{-3}	M_w/M_n	M_w(GPC) × 10^{-3}	M_w/M_n
C-2	404	3.1	408	3.5
C-4	200	3.2	220	3.5
C-6	58	3.6	61	3.8

Table V
Results When the D_2O/H_2O Ratio Matches the Whole Swollen Particle

sample ID	molar swelling ratio	latex scaling ratio (R_g/a_w)	extent of segregation (N_s)
S-2-a	1.0	0.48	43
S-2-b	3.0	0.37	93

Table VI
Results When the D_2O/H_2O Ratio Matches Styrene

sample ID	molar swelling ratio	latex scaling ratio (R_g/a_w)	extent of segregation (N_s)
H-6-a	1.0	0.17	1820
H-6-b	2.0	0.15	1330
H-6-c	3.0	0.14	1220

As shown in Table V, one sample (S-2) of the series S was prepared additionally in the swollen state, but the molar swelling ratio was increased to 3. Accordingly, the composition of the swollen latex particles was 25/75 mol % of deuterated polystyrene and protonated styrene monomer. For this sample, a mixture of D_2O/H_2O (44.4/55.6 mol %) was used to match the average contrast factor of the swollen latex particle.

The blanks were synthesized in exactly the same way as mentioned above, except that mixtures of deuterated and protonated styrene monomers were used. The blank seed was a statistical copolymer of deuterated and protonated styrene, which was swollen with the same monomer mixture.

Contrast Matching to the Second Monomer. Series H Samples. The series H samples were prepared in the swollen state like the series S samples, but the molar swelling ratio was varied from 1 to 3 to have different particle sizes, keeping the same molecular weight of polymer I; see Table VI. In this case, the average contrast factor of the aqueous medium was matched to that of the added protonated styrene monomer, with a mixture of D_2O/H_2O of 26/74 mol %. The blanks were prepared with 100% protonated styrene. The blank seed composed of protonated polystyrene was swollen with protonated styrene monomer.

Results

All SANS measurements were done on diluted latex dispersions of 5% solid content to avoid the interparticle interference and maximize the signal-to-noise ratio.[36] Measurements were made in the range of 25–50 mol % deuterated polymer, based on solid content, in order to minimize the beam time requirements. Figure 1 shows a Debye plot of the raw data for sample S-1. Three theoretical curves based on single-chain scattering are shown for comparison. These are the $P_1(\mathbf{K})$ scattering curves based on (1) the GPC M_w and the corresponding value of R_g; (2) the actual $(d\Sigma/d\Omega)(0)$ value and the R_g value from (1); and (3) the actual $(d\Sigma/d\Omega)(0)$ value and the experimental R_g for the equivalent sphere. The fit of the three possibilities to the experimental data is so poor that the data cannot be analyzed by single-chain scattering relationships. The strong scattering intensities at low angles ($K < 0.01$ Å^{-1}) reflect a possible molecular segregation inside the latex particle.

Figure 2 shows a Guinier plot in terms of ln $(d\Sigma/d\Omega)$ vs $\mathbf{K}^2$. A straight line was obtained through the low angles based on Guinier approximation. The intercept value, $d\Sigma/d\Omega(0)$, proportional to the number of segregated

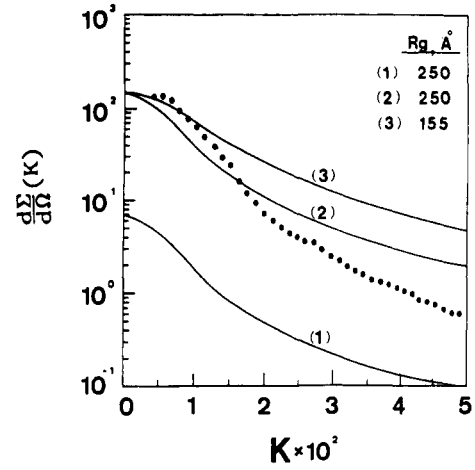

Figure 1. Debye random-coil fitting with experimental data for sample S-1: (●) SANS raw data, (—) theoretical $P_1(\mathbf{K})$ scattering curve.

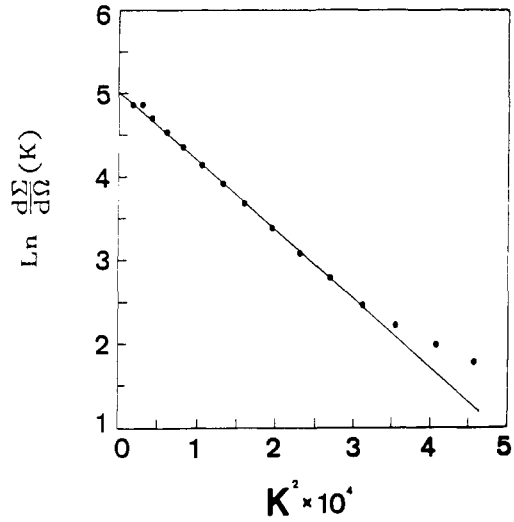

Figure 2. Guinier plot at low-angle portions for sample S-1.

molecules, was determined by extrapolation to zero angle with a least-squares fitting; and the equivalent sphere radius, R, of the segregated region was determined from the slope. For sample S-1, $(d\Sigma/d\Omega)(0)$ yields M_w^{SANS} = 1.7×10^7 g/mol, and for $M_w^{GPC} = 8.0 \times 10^5$ g/mol, N_s = 21. The radius R value, as determined from the slope, was 200 Å. These values were used to obtain the theoretical spherical scattering curve for $P_2(\mathbf{K})$ in Figure 3. Also plotted are the experimental data. Agreement is only obtained at low angles, although slight shoulders, matching theory, can be seen. However, those shoulders are at the limit of experimental error.

SANS results for the S series in the swollen state are listed in Table II. None of SANS data gave single-chain characteristics on the basis of uniform molecular mixing, indicating that there exists a concentration gradient of the seed polymer and the added monomer inside the latex particle in the swollen state. The extent of segregation is seen to vary according to the ratio R_g/a_w of chain radius of gyration to the particle radius a_w with both numerator and denominator calculated as weight-average values.

SANS data in Table III reveal how the extents of segregation vary during and after the polymerization of the added monomer in the second stage. The quantity N_s in Tables II and III was plotted against the ratio R_g/a_w in Figure 4. Figure 4 shows that the extent of segregation is highest in the swollen state, decreasing somewhat as polymerization proceeds. However, regardless of the

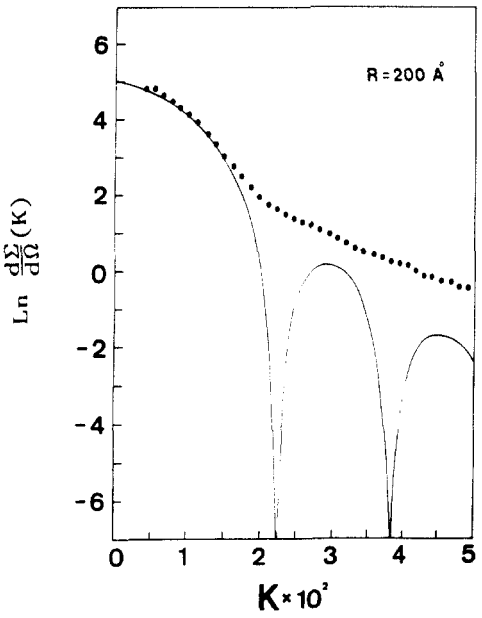

Figure 3. Spherical scattering fitting with experimental data for sample S-1: (●) SANS raw data, (—) theoretical $P_2(\mathbf{K})$ scattering curve.

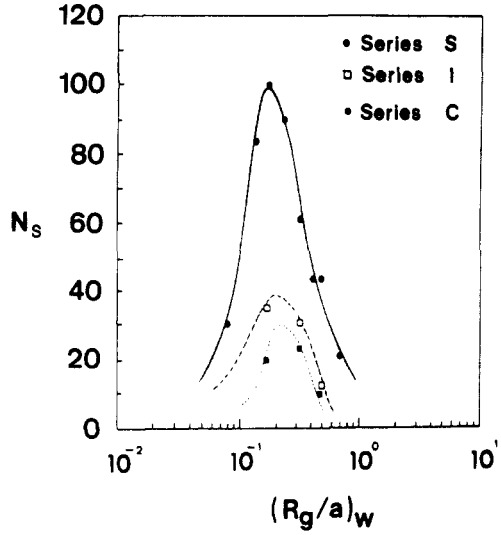

Figure 4. Effects of the latex scaling ratio on the development of supramolecular structure during second-stage polymerization: (●) 0% conversion in the swollen state, (□) 42% conversion, (■) complete conversion (>98%).

second-stage conversions, the quantity N_s goes through a maximum at R_g/a_w about 0.2.

The existence of a maximum in the segregation when R_g/a_w is about 0.2 is also shown in Tables V and VI, by increasing the swollen particle size at fixed molecular weights. Sample S-2 in Table V shows that the extent of segregation increases as the ratio R_g/a_w decreases, when the ratio R_g/a_w is larger than 0.2. Sample H-6 in Table VI shows that the extent of segregation decreases as the ratio R_g/a_w decreases, when the ratio R_g/a_w is smaller than 0.2. These results can be visualized in Figure 4, by increasing or decreasing the ratio R_g/a_w in regions higher or lower than 0.2.

Latex–Water Interface as a Repulsive Wall

Joanny et al.[37] and de Gennes[11,12] discussed the concentration profile of confined polymer solutions between two flat walls and in cylindrical tubes by considering the interface–polymer interactions. The interface constitutes a repulsive wall, leading to a depletion layer near the wall such that the concentration of polymer vanishes at an ideal surface and increases to the bulk concentration in the interior. Cassasa and co-workers[8,9] computed the loss of conformational entropy in terms of the average chain fractions remaining inside the confined boundary. These concepts have already been applied to such problems as gel permeation chromatography and the coagulation of latexes. These same ideas, using spherical geometry, will now be applied to the interior structure of latexes.

The segment density profile of the polymer chains inside the swollen particle can be estimated by applying the work of Cassasa on polymer segment distribution in the presence of a repulsive wall.[8-10] The required chain statistics is given by the diffusion equation

$$\frac{\partial P_N(r)}{\partial N} = \frac{b^2}{6}\nabla^2 P_N(r) \tag{10}$$

$$R_g^2 = Nb^2/6 \tag{11}$$

where $P_N(r)\,dr$ is the probability for finding a random flight of N steps within a spherical differential volume element dr at a distance r from the center and b^2 is the mean-square step length.

The first step in finding the segment density distribution in a confining sphere is to find the probability, $P_N(r/r',a)$, that a chain starts at r' and ends at r such that the chain residues within a nonperturbing boundary defined by the surface of a sphere with radius a. The necessary boundary condition is that the probability $P_N(r/r',a)$ vanishes over the surface of the particles, which in this case represents the repulsive wall.

As discussed by Cassasa,[9] the first step is equivalent to calculating the temperature at a radius r at time t due to an instantaneous spherical surface heat source of strength unity generated at a radius r' at $t = 0$, the isotropic solid being initially at zero temperature and the surface being kept at zero temperature for all t. From the classical theory of heat conduction, $P_N(r/r',a)$ for a sphere of radius a is given by[39]

$$P_N(r/r',a) = \frac{1}{2\pi a r' r}\sum_{n=1}^{\infty}\sin\frac{n\pi r'}{a}\sin\frac{n\pi r}{a}\exp\{-n^2\pi^2(R_g/a)^2\} \tag{12}$$

To obtain the segment density profile as a function of the distance s from the center of the spherical particle, we look at a chain starting from an arbitrary point r', reaching s in m steps and extending to an arbitrary point r in another $n - m$ steps.

The probability that the two subchains of m and $n - m$ segments do not touch the surface at a is the product of the individual probabilities. This probability, which is expressed as the number of mth segments per unit volume at s, is also the mth segment density profile, $C_m(s)$, for all the chains in the particle and can be formally expressed as

$$C_m(s) = 16\pi^2\int_0^a r^2 P_m(r'/s,a)\,dr\int_0^a r^2 P_{n-m}(r'/s,a)\,dr \tag{13}$$

Using the probabilities defined in eq 12 and integrating over r yields

$$C_m(s) = \frac{4a^2}{\pi^2 s^2}\sum_{p=1}^{\infty}\sum_{q=1}^{\infty}\frac{(-1)^{p+q}}{pq}\sin\left(\frac{p\pi s}{a}\right)\sin\left(\frac{q\pi s}{a}\right)\times \exp\left\{\frac{-\pi^2 b^2}{6a^2}[p^2 m + q^2(n-m)]\right\} \tag{14}$$

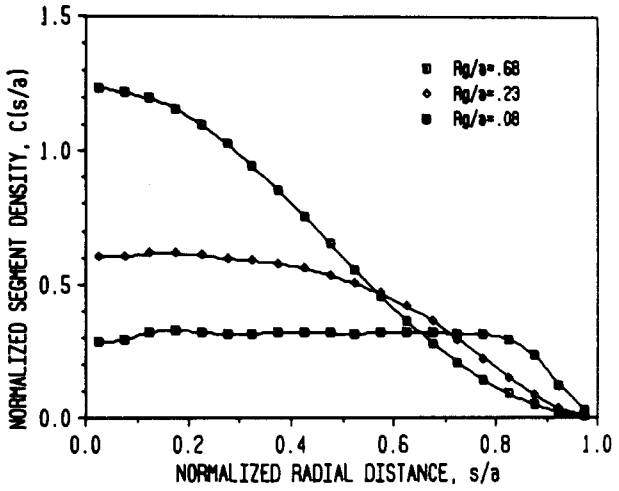

Figure 5. Normalized segment density profile of the polymer chains in a sphere of radius a.

Introducing the variable

$$u = m/n \text{ such that } 0 \le u \le 1 \tag{15}$$

and the dimensionless or normalized radial distance s/a, we can rewrite eq 14 in the form

$$C_u(s/a) = \frac{4a^2}{\pi^2 s^2}\sum_{p=1}^{\infty}\sum_{q=1}^{\infty}\frac{(-1)^{p+q}}{pq}\sin\left(\frac{p\pi s}{a}\right)\sin\left(\frac{q\pi s}{a}\right)\times \exp\left\{\frac{-\pi^2 R_g^2}{a^2}[p^2u + q^2(1-u)]\right\} \tag{16}$$

To obtain the average segment density profile in the particle, one must average $C_u(s/a)$ over all the segments in the chain:

$$\bar{C}(s/a) = \int_0^1 C_u(s/a)\,du \tag{17}$$

In order to compare profiles at different values of R_g/a, it is necessary to normalize the segment density profile such that

$$\int_0^1 4\pi(s/a)^2\bar{C}(s/a)\,d(s/a) \tag{18}$$

accounts for all the segments in the particle. Thus we can express the normalized segment density distribution, $C(s/a)$, as

$$C(s/a) = \frac{\bar{C}(s/a)}{4\pi\int_0^1 (s/a)^2\bar{C}(s/a)\,d(s/a)} \tag{19}$$

such that

$$4\pi\int_0^1 (s/a)^2 C(s/a)\,d(s/a) = 1 \tag{20}$$

With the lowest, intermediate, and largest values of R_g/a from Table II the normalized segment density distributions were calculated and are shown in graphical form in Figure 5. The curves at low R_g/a show a uniform sigmoidal density from the center of the sphere toward the surface, dropping off only close to the surface. Near the particle center the errors may be appreciable, making the segment density values questionable.

The segment density distribution is very sensitive to an R_g/a ratio between 0.08 and 0.68, the experimental range studied in this work. At the lower value uniform molecular arrangement is predicted except very near the wall, while at higher values the segments seem to be depleted further from the surface.

This explains that molecular segregation inside the swollen particle depends only on the ratio R_g/a. This corresponds to the SANS results, especially in the lower regions of the ratio R_g/a below the maximum point in Figure 4. As the ratio $R_g/a \to 0$, uniform molecular mixing is obtained because the repulsive wall effect disappears in this limiting condition.

Discussion

Should Segregation in Latexes Always Exist?

SANS results indicate the extent of segregation decreases as the polymerization of the added monomer continues to complete conversion; see Figure 4. Self-diffusion and other mechanisms are thought to affect the extent of segregation during the second-stage polymerization. Several cases can be explained on the basis of the result.

1. Owing to the presence of unreacted monomer inside partially polymerized latexes, the glass transition temperature of polymer solution is lower than the reaction temperature, self-diffusion being facilitated. This tends to decrease segregation. However, as the polymerization proceeds to complete conversion, the polymer solution may become more glassy, decreasing the effect of chain diffusion.

Therefore, the supramolecular structure cannot be expected in a fully polymerized latex having a glass transition temperature lower than the reaction temperature. The polymer chains inside the particle will be uniformly mixed by self-diffusion during the polymerization.

As an interesting side point, one must consider the molecular weight distribution. According to the above model, short chains will prefer positions close to the surface, while longer chains will be in the interior; see Figure 5. This could possibly influence the physical and mechanical behavior of latex films that are incompletely interdiffused during molding.

Of course, in the neat molten latexes, with mixing of the deuterated and undeuterated species of the same molecular weights and distribution, there can be no concentration gradients because of the requirement of uniform density.

An important determinant of self-diffusion is the molecular weight of the polymer chains, because the self-diffusion of linear chains is inversely proportional to the square of molecular weight. At very low molecular weights, the concentration gradient of polymer chains inside the swollen particle may disappear rapidly due to self-diffusion during the polymerization. This effect is different from the small region of concentration gradient expected at a repulsive wall.

2. If the polymer becomes insoluble in monomer, then polymer chains move according to the phase-separation mechanism. An example is the polymerization of vinyl chloride via latex formation.

3. If the polymer crystallizes during the polymerization, another type of supramolecular structure will appear.

4. If the polymer is attracted to the interface, perhaps by water-soluble mers, or ionic groups, then polymer chains will be arranged along the particle surface. An example is the polymerization of sodium sulfonated styrene via latex formation.

By contrast, when should segregation of a core–shell nature be expected? The data to date provide several suggestions: (1) that the relaxed polymer chain dimensions be a reasonable fraction of the latex size; (2) that the polymer be soluble in the monomer; and (3) that a reasonable fraction of monomer remain in the system at the time of measurement.

With regard to this last, the extent of segregation remaining after 100% conversion depends on the glass transition temperature, as discussed elsewhere.

Ionic End Groups. Also, the effect of ionic chain end groups on the extent of segregation should be considered. With persulfate initiation, it has been reported that 1.0–1.6 surface sulfate end groups for each polystyrene molecule are produced, the other end groups being buried. However, a polymer chain maintained near the surface cannot occupy a random-coil conformation because the repulsive wall of the particle–water interface. Therefore, in this case, the polymer chains inside the swollen latex tend to be centered in the particle like a core–shell structure, with their sulfate end groups at the surface, whereas if 2.0 sulfate end groups per polystyrene molecule were on the surface of the particle and the particle size were large enough, about or above 0.5 μm, then inverse core–shell morphology might be expected.

The above assumes every chain has at least one, maybe two, sulfate end groups, depending on the ratio of termination by combination vs termination via disproportionation. This is true when no chain-transfer agent is employed. In the present case, carbon tetrachloride was used to control the molecular weight at various levels. At zero concentration of carbon tetrachloride, a weight-average molecular weight of 800 000 g/mol was obtained. For the highest carbon tetrachloride concentration employed, 10% by weight based on monomer, a weight-average molecular weight of 20 000 was obtained; see Table I. Thus, the larger number of chains for the lower molecular weight samples contain no ionic end groups and are relatively free to position themselves anywhere in the latex particle.

As shown in Figure 4, the extent of segregation, N_s, goes through a maximum, depending on the ratio R_g/a_w. It should be pointed out why a maximum segregation exists inside the latex particles at a R_g/a_w of about 0.2.

Case of Large Chains. When a polymer chain with a large ratio $\bar{r}/D$ ($\gg$1) is constrained in a cylindrical tube of diameter D, contacting with a repulsive wall, de Gennes[10] showed that the chain end-to-end distance parallel to the tube axis is equivalent to that in the relaxed state; that is, constraint does not affect the components of the random motion parallel to the tube axis. In latex particles with spherical geometry, Linne[18,19] found that the polymer chains of very high molecular weights were constrained in the relatively small latex particles by a factor of 2–4 from the relaxed chain dimensions, leading to uniform molecular mixing inside the particle. Long chains cannot be arranged inside a small particle without touching a repulsive wall at the particle–aqueous interface. At very high molecular weights, entropic forces of isotropic compression become dominant and apparently force molecular mixing inside the particle.

A maximum segregation inside the particle exists when the repulsive forces from the interface are balanced with the entropic forces of mixing.

Kinetics of Emulsion Polymerization. Most researchers accept that the main polymerization loci in latexes are uniformly swollen particles at equilibrium with the aqueous phase.[40,41] Besides temperature, initiator concentration, etc., kinetic models depend solely on the monomer concentration in the particles.

The present study indicates that the monomer concentration depends additionally on both polymer molecular weight and particle diameter in terms of the ratio R_g/a_w, so that the classical uniformity criterion is not always satisfied. Consequently, there is a significant regime of practical importance in which a polymer-rich core and a monomer-rich shell exist. The kinetic interpretations of experimental data have generated significant controversy,[1,5] while others have reconciled their kinetic data in terms of an existing monomer-rich shell.[42] Without having systematic kinetic data available in this regime, the authors can only speculate on the kinetic effect of a monomer-rich shell during polymerization.

a. Batch Polymerization. During the constant-rate period, monomer is supplied to the particles from the monomer droplets in the aqueous phase. With persulfate initiator, the initiation takes place in the water phase and the oligomeric radical is captured by the particle. This free radical encounters a monomer-rich shell environment.

The polar end stays at the particle surface, and without chain transfer, the polymer preferentially propagates into the more monomer-rich parts of the particle, reducing the monomer concentration gradient. The gradient quickly converges to a limiting equivalent shell thickness and concentration, which is then maintained by the constraint of the "repulsive wall effect" for the growing segments. On the other hand, as described above, the larger number of chains are formed through chain transfer and may have no ionic end group such as sulfate. Thus, several forces are constantly interplaying, producing opposing effects.

b. Semibatch. In a semibatch system, the monomer feed rate is normally larger than the reaction rate and therefore monomer builds up in the reactor. Wessling[42] has shown that this monomer buildup is equal to the monomer residing in the constant thickness shell layer of the particle. This picture is consistent with conclusions based on the current experiments.

In summation, the kinetics of emulsion polymerization should be modified to allow for the repulsive wall effect and concomitant polymer chain segregation within the latex particle.

Two additional points should be mentioned:

1. The polystyrene in this paper has M_n up to 2.58 × 10^5 g/mol. It should be noted that the Flory–Huggins free energy of mixing expression for a heterodisperse system requires the number-average degree of polymerization.[43] Bates et al.[44,45] found excess SANS intensities in polystyrene mixtures due to H–D segregation; it is possible that a slight effect is contained herein. However, calculations for this molecular weight show an upper critical solution temperature of about 150 K, well below the range of current interest, 290 K and above.

2. Ullman[46] has given corrections for data where $\mathbf{K}R_g > 1$. In the present case, the corrections were below 10% and were thus ignored.

Conclusions

The present SANS experiments on polystyrene latexes show that the development of supramolecular structure arises from a concentration gradient in the swollen state, between seed polymer and added monomer. The extent of segregation is the highest in the swollen state, decreasing as the polymerization of monomer continues. Molecular segregation inside the latex particles is controlled by two thermodynamic factors. One is the loss of conformational entropy due to a repulsion at the particle–aqueous interface, as in the case of polymer solutions in contact with an aqueous phase.

The theoretical segment density profile of the polymer chains is high in the central region of the particle, vanishing quadratically at the surface. This supports a polymer-rich core surrounded by a monomer-rich shell. Both experimental evidence and theoretical analysis indicate

that the extent of segregation depends on the ratio R_g/a_w. At very low molecular weights, the repulsive forces from the interface diminish in scope. The entropic forces dominant at very high molecular weights and small particles cause mixing forces due to constraining. These two opposing forces explain why a maximum segregation exists at a ratio of R_g/a_w of approximately 0.2.

Acknowledgment. We thank the National Science Foundation for support through Grant No. CBT-8512923. The SANS experiments were performed at the National Bureau of Standards, funded by NSF Grant No. DMR-7724458 through interagency agreement No. 40-637-77 with DOE. We thank Dr. C. J. Glinka of the Polymer Division, National Bureau of Standards, for his many helpful discussions and assistance with the SANS experiments.

Appendix I

The classical relationship for scattering intensity, $I(q)$, for homopolymers at low concentration c, using the single contact approximation between different chains, was derived by Zimm (A1) where K_0 is a constant dependent

$$I(q) = K_0cMP(q) - 2A_2McP^2(q) \tag{A1}$$

on the apparatus and the type of radiation, M is polymer molecular weight, A_2 is the second virial coefficient, and q is the magnitude of the wave vector, which can be written as

$$q = (4\pi/\lambda)\sin(\theta/2) \tag{A2}$$

λ is the wavelength of the incident radiation and θ is the scattering angle. $P(q)$ is the normalized single-chain form factor, which is defined

$$n^2P(q) = g(q) \tag{A3}$$

in which $g(q)$ is the distribution function for the vector distance between all the monomer pairs on the same chain and n is the number of monomers per chain. Benoit has looked at the more general problem of scattering from a polymer solution at any arbitrary concentration (A2), and he derived, for higher order contacts, a neutron scattering model for a mixture of ordinary and deuterated polymers in a solvent solution

$$I(q) = x(1-x)(a-b)^2Ng(q) + \bar{a}^2\left[Ng(q) - \frac{N^2g(q)^2v(c)}{1+v(c)nG(q)}\right] \tag{A4}$$

where x is the fraction of deuterated chains, N is the number of polymer chains in a unit volume of solution, a and b are the coherent scattering lengths corresponding to the deuterated and protonated monomers, and $v(c)$ is the excluded volume between pairs of monomers. The average scattering length is defined as

$$\bar{a} = (a-s)x + (b-s)(1-x) \tag{A5}$$

where s is the coherent scattering length of the solvent. In the semidilute regime, following the arguments of Benoit, one can write the expression for the excluded volume

$$v(c) = \frac{2}{N_t}\left[\frac{1}{2} - \chi + \frac{\phi_2}{2\phi_1}\right] \tag{A6}$$

where N_t is the total number of solvent and monomer molecules, χ is the polymer solvent interaction parameter, and ϕ_1 and ϕ_2 are the solvent and polymer fractions, respectively. There are two experimental conditions to consider in this paper: (a) deuterated polymer in protonated monomer solvent, and (b) protonated and deuterated polymer in the presence of protonated monomer. In the first case $x = 0$ and the scattering equation reduces to

$$I(q) = (a-s)^2\left[Ng(q) - \frac{N^2g(q)^2v(c)}{1+v(c)Ng(q)}\right] \tag{A7}$$

which can be written in the form

$$(a-s)^2I^{-1}(q) = \frac{1}{Ng(q)} + v(c) \tag{A8}$$

Since the excluded volume is related to the interaction parameter and solvent swelling of the particle, the excluded volume for the blank and the sample will be very close. For this reason, one may argue that the blank correction has reduced the effect of the excluded volume. If so, the Zimm plot will indeed yield the SANS molecular weight and radius of gyration. In the second case, when some deuterated polymer is present and the average scattering length is adjusted to the theoretical zero, the scattering expression becomes

$$I(q) = x(1-x)(a-b)^2Ng(q) \tag{A9}$$

which again can be written

$$(a-b)^2(1-x)xI^{-1}(q) = \frac{1}{nG(q)} \tag{A10}$$

to yield the molecular weight and radius of gyration from the Zimm analysis.

In addition, the numerical values of N_s bear comparison to similar values delineated by Linne et al.[18] and Yang et al.,[20] as well as shown in Table III of this work. In each case, noting the value of the ratio R_g/a_w, similar values were obtained. This supports the above finding that the relations can be used continuously from a deuterated polymer in a protonated monomer solvent to the blend of the two polymers.

References and Notes

(1) Grancio, M. R.; Williams, D. J. *J. Polym. Sci.* **1970**, *A18*, 2617.
(2) Grancio, M. R.; Williams, D. J. *J. Polym. Sci.* **1970**, *A18*, 2733.
(3) Keusch, P.; Williams, D. J. *J. Polym. Sci., Polym. Chem. Ed.* **1973**, *11*, 143.
(4) Keusch, P.; Prince, J.; Williams, D. J. *J. Macromol. Sci., Chem.* **1973**, *A7*, 623.
(5) Gardon, J. L. *J. Polym. Sci. Polym. Chem. Ed.* **1973**, *11*, 241.
(6) Napper, D. H. *J. Polym. Sci.* **1971**, *A19*, 2089.
(7) Friis, N.; Hamielec, A. E. *J. Polym. Sci., Polym. Chem. Ed.* **1973**, *11*, 3321.
(8) Casassa, E. F. *J. Polym. Sci., Polym. Lett. Ed.* **1967**, *5*, 773.
(9) Casassa, E. F.; Tagami, Y. *Macromolecules* **1969**, *2*, 14.
(10) de Gennes, P.-G. In *Scaling Concepts in Polymer Physics*; Cornell University Press: Ithaca, NY, 1979.
(11) de Gennes, P.-G. *Macromolecules* **1981**, *14*, 1637.
(12) de Gennes, P.-G. *Adv. Colloid Interface Sci.* **1987**, *27*, 189.
(13) Richmond, P.; Lal, M. *Chem. Phys. Lett.* **1974**, *24*, 594.
(14) Allain, C.; Ausserre, D.; Rondelez, F. *Phys. Rev. Lett.* **1982**, *49*, 1694.
(15) Higgins, J. S.; Stein, R. S. *J. Appl. Cryst.* **1978**, *11*, 346.
(16) Macconachie, A.; Richards, R. W. *Polymer* **1978**, *19*, 739.
(17) Sperling, L. H. *Polym. Eng. Sci.* **1984**, *24*, 1.
(18) Linne, M. A.; Klein, A.; Sperling, L. H. *J. Macromol. Sci., Phys.* **1988**, *B27* (2 & 3), 181.
(19) Linne, M. A.; Klein, A.; Sperling, L. H. *J. Macromol. Sci., Phys.* **1988**, *B27* (2 & 3), 217.
(20) Yang, S. I.; Klein, A.; Sperling, L. H. *J. Polym. Sci., Polym. Phys. Ed.* **1989**, *27*, 1649.
(21) Hasan, S. H. *J. Polym. Sci., Polym. Chem. Ed.* **1982**, *20*, 3031.
(22) Bates, F. S.; Cohen, R. E.; Berney, C. V. *Macromolecules* **1982**, *15*, 589.
(23) Bates, F. S.; Berney, C. V.; Cohen, R. E.; Wignall, G. D. *Polymer* **1982**, *24*, 519.

(24) Berney, C. V.; Cohen, R. E.; Bates, F. S. *Polymer* **1982**, *23*, 1222.
(25) Berney, C. V.; Kofinas, P.; Cohen, R. E. *Polym. Commun.* **1986**, *27*, 330.
(26) Benoit, H.; Benmouna, D. M. *Macromolecules* **1984**, *17*, 535.
(27) (a) Benoit, H.; Wu, W.; Benmouna, D. M.; Mozer, B.; Bauer, B.; Lapp, A. *Macromolecules* **1985**, *18*, 986. (b) King, J. S.; Boyer, W.; Wignall, G. D.; Ullman, R. *Macromolecules* **1985**, *18*, 709.
(28) Ottewill, R. H. In *Colloid Dispersions*; Goodwin, J., Ed.; Special Publication No. 43, Royal Society of Chemistry: London, 1982; p 143.
(29) O'Reilly, J. M.; Melpolder, S. M.; Fisher, L. W.; Ramakrishnan, V.; Wignall, G. D. *Polym. Prepr. (Am. Chem. Soc., Div. Polym. Chem.)* **1983**, *24*, 407.
(30) Wai, M. P.; Gelman, R. A.; Hoerl, M. G.; Fatica, R. H.; Wignall, G. D. *Polymer* **1987**, *28*, 918.
(31) Hasegawa, H.; Tanaka, H.; Hashimoto, T.; Han, C. C. *Macromolecules* **1987**, *20*, 2120.
(32) Matsushita, Y.; Nakao, Y.; Saguchi, R.; Mori, K.; Choshi, H.; Muroga, Y.; Noda, I.; Nagasawa, M.; Chang, T.; Glinka, C. J.; Han, C. C. *Macromolecules* **1988**, *22*, 1802.
(33) Glatter, O.; Kratky, O. In *Small Angle X-ray Scattering*; Academic Press: London, 1982.
(34) Wignall, G. D.; Ballard, D. G. M.; Schelten, J. *Eur. Polym. J.* **1974**, *10*, 861.
(35) Sperling, L. H. In *Introduction to Physical Polymer Science*; Wiley-Interscience: New York, 1986.
(36) Higgins, J. S.; Tomlins, P. E.; Dawkins, J. V.; Maghami, G. G.; Shakir, S. A. *Polym. Commun.* **1988**, *29*, 122.
(37) Joanny, J. F.; Leibler, L.; de Gennes, P.-G. *J. Polym. Sci., Polym. Phys. Ed.* **1979**, *17*, 1073.
(38) Jones, J. S.; Richmond, P. *J. Chem. Soc., Faraday Trans. 2* **1977**, *73*, 1062.
(39) Carslaw, H. S.; Jaeger, J. C. In *Conduction of Heat in Solids*, 2nd ed.; Oxford University Press: London, 1959.
(40) Russel, G. T.; Napper, D. H.; Gilbert, R. G. *Macromolecules* **1988**, *21*, 2133.
(41) Maxwell, I. A.; Sudol, E. D.; Napper, D. H.; Gilbert, R. G. *J. Chem. Soc., Faraday Trans. 1* **1988**, *84* (9), 3107.
(42) Wessling, R. A.; Gibbs, D. S. *J. Macromol. Sci., Chem.* **1973**, *A7* (3), 647.
(43) Flory, P. J. *Principles of Polymer Chemistry*; Cornell University Press: Ithaca, NY, 1953; p 513.
(44) Bates, F. S.; Wignall, G. D. *Macromolecules* **1986**, *19*, 932.
(45) Bates, F. S. *J. Appl. Cryst.* **1988**, *21*, 681.
(46) Ullman, R. *J. Polym. Sci., Polym. Phys. Ed.* **1983**, *23*, 1477.

Registry No. Styrene, 100-42-5; polystyrene, 9003-53-6.